Science Advances
AAAS

Supplementary Materials for

A pleiotropic hypoxia-sensitive *EPAS1* enhancer is disrupted by adaptive alleles in Tibetans

Olivia A. Gray *et al.*

Corresponding author: Olivia A. Gray, oagray@uchicago.edu; Anna Di Rienzo, dirienzo@bsd.uchicago.edu

Sci. Adv. **8**, eade1942 (2022)
DOI: 10.1126/sciadv.ade1942

The PDF file includes:

Other Supplementary Material for this manuscript includes the following:

Supplementary Text

Mouse RNA-seq analyses

Comparison of transcriptional patterns for genes expressed across tissues revealed correlations amongst almost all tissues. An exception was observed for left ventricle (LV) where the extent of differential expression across genotypes was only loosely correlated with that of other tissues or showed an inverse correlation (up-regulated in left ventricle and down-regulated in right ventricle). Although we were unable to conclusively identify the cause of this artifactual observation, we hypothesize that timing and order of dissection in the context of a hypoxia-responsive enhancer played a role. Left ventricle was the final of the seven tissues to be dissected and frozen, and therefore had the longest exposure to normoxia, particularly in the second mouse to be euthanized and dissected. Nevertheless, inclusion or exclusion of data from this tissue did not substantially alter the results of downstream analyses. The differences in the expression patterns observed in the analysis including or omitting the LV data were negligible, as shown in fig. S6.

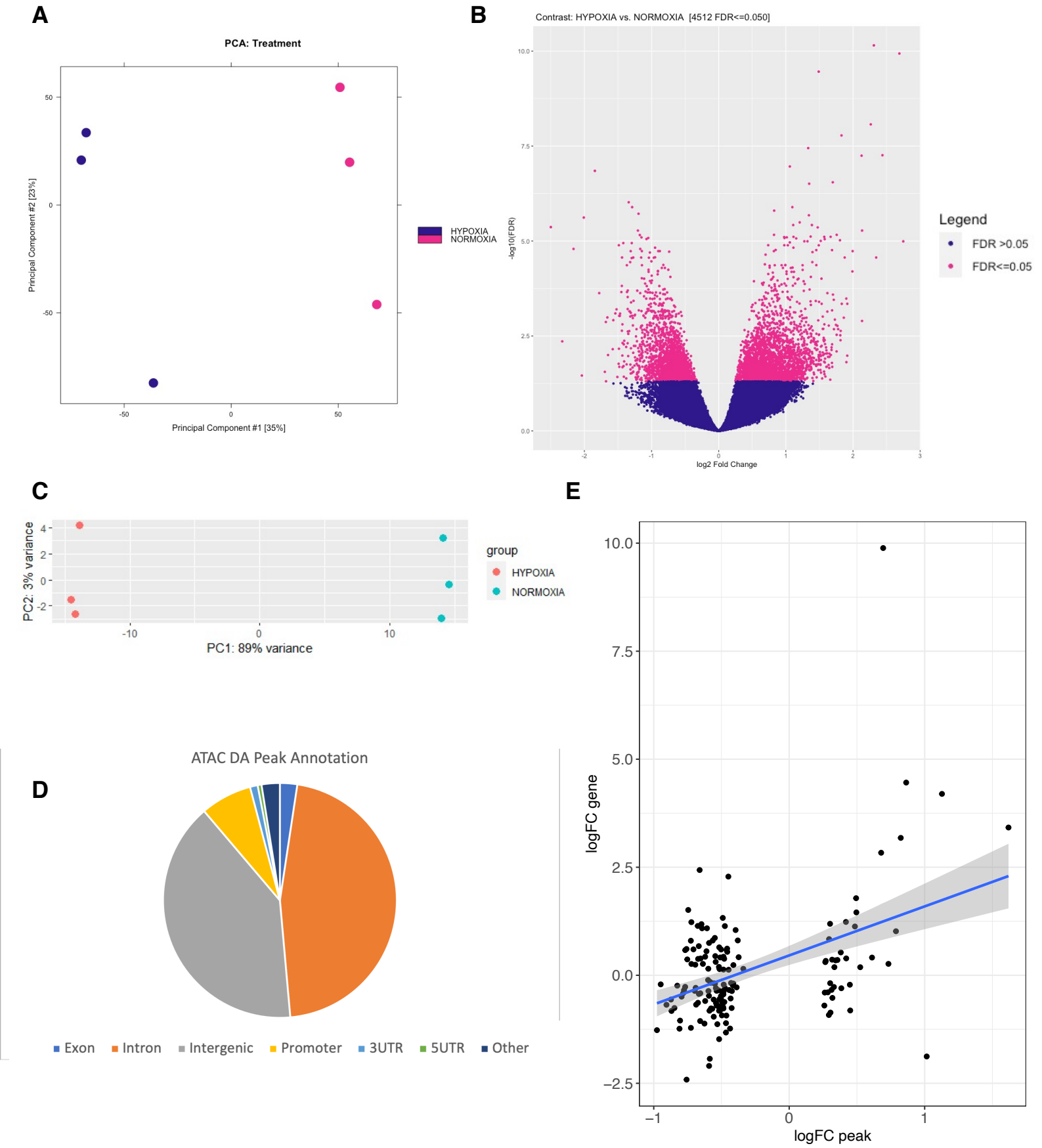
A
PCA: Treatment
Principal Component #2 [23%]
Principal Component #1 [35%]
HYPOXIA
NORMOXIA
B
Contrast: HYPOXIA vs. NORMOXIA [4512 FDR<=0.050]
-log10(FDR)
log2 Fold Change
Legend
FDR >0.05
FDR<=0.05
C
PC2: 3% variance
PC1: 89% variance
group
HYPOXIA
NORMOXIA
D
ATAC DA Peak Annotation
Exon
Intron
Intergenic
Promoter
3UTR
5UTR
Other
E
logFC gene
logFC peak
F
ATAC-seq peaks
EPAS1
ENH4
ENH6
ENH5
ENH8

Fig. S1. Summary data for ATAC-seq and RNA-seq analyses in HAEC's exposed to 24 hours of normoxia or hypoxia (1% O_2). (A) Principal component analysis of the ATAC-seq data labeled by treatment condition. (B) Volcano plot of differentially accessible ATAC-seq peaks. (C) Principal component analysis of RNA-seq data labeled by treatment condition. (D) Annotation of differentially accessible ATAC-seq peaks. (E) Change in chromatin accessibility at ATAC-seq peaks plotted against the change in transcript levels for DE genes (padj<0.05) with a peak in their promoter. F) Position of ATAC-seq peaks within the *EPAS1* gene relative to enhancer elements with differential activity.

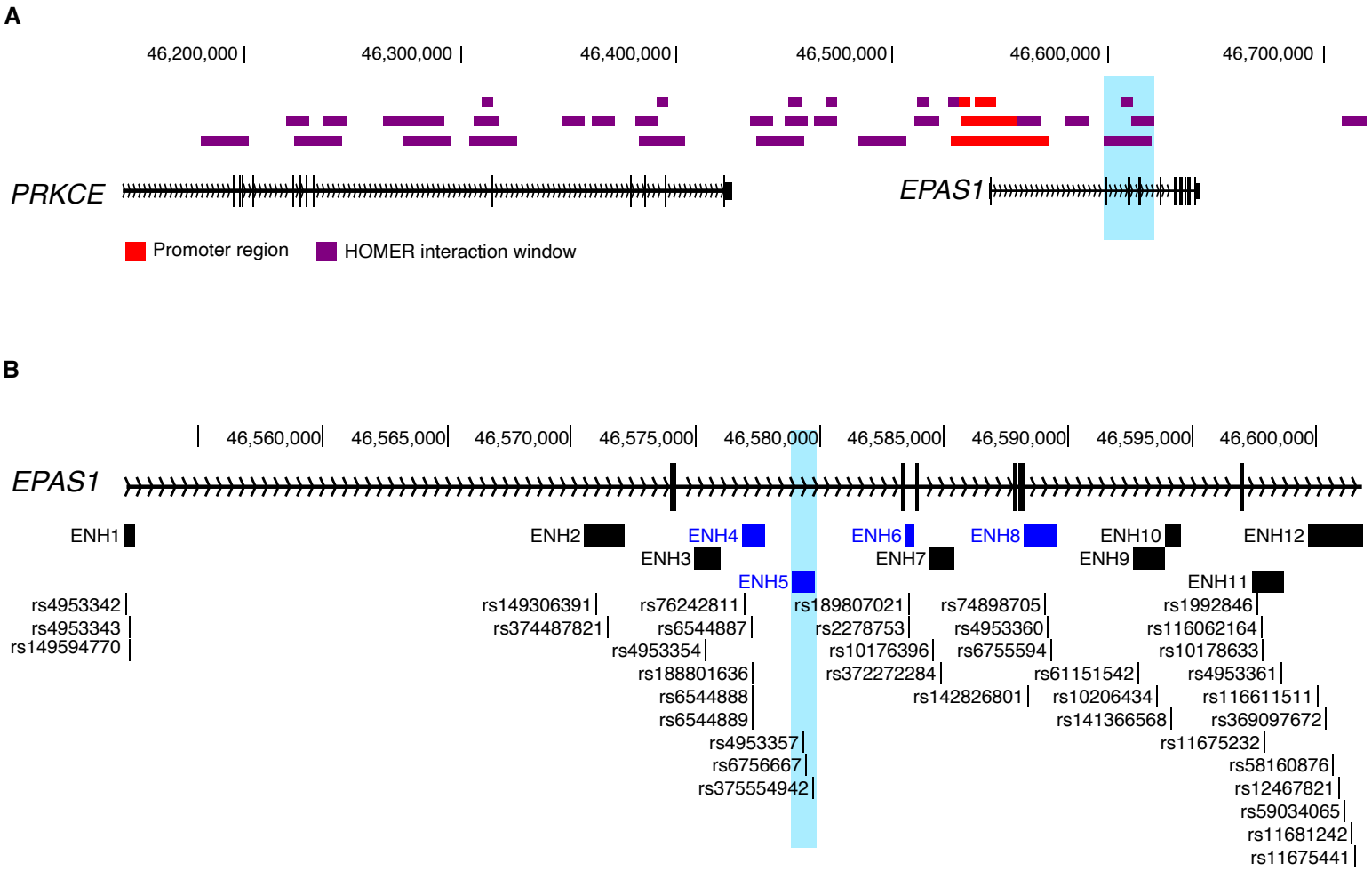
A
46,200,000
46,300,000
46,400,000
46,500,000
46,600,000
46,700,000
PRKCE
EPAS1
Promoter region
HOMER interaction window
B
46,560,000
46,565,000
46,570,000
46,575,000
46,580,000
46,585,000
46,590,000
46,595,000
46,600,000
EPAS1
ENH1
ENH2
ENH3
ENH4
ENH5
ENH6
ENH7
ENH8
ENH9
ENH10
ENH11
ENH12
rs4953342
rs4953343
rs149594770
rs149306391
rs374487821
rs76242811
rs6544887
rs4953354
rs188801636
rs6544888
rs6544889
rs4953357
rs6756667
rs375554942
rs189807021
rs2278753
rs10176396
rs372272284
rs142826801
rs74898705
rs4953360
rs6755594
rs61151542
rs10206434
rs141366568
rs1992846
rs116062164
rs10178633
rs4953361
rs116611511
rs369097672
rs11675232
rs58160876
rs12467821
rs59034065
rs11681242
rs11675441

Fig. S2. Genetic architecture of the *EPAS1* locus. (**A**) All HOMER interaction windows for the *EPAS1* promoter ascertained, from top to bottom, at 5kb, 10kb, and 20kb windows. The blue highlighted region encompasses the union of the three distal overlapping interaction windows in EPAS1, as described in the text. (**B**)Boxes below the *EPAS1* gene show the locations of the luciferase reporter constructs used to test for allelic effects. Blue regions show enhancer regions with significant allelic effects ($p < 0.05$) . Black tick marks underneath indicate the position and rsID of all SNPs tested in enhancer assays (listed in table S2).

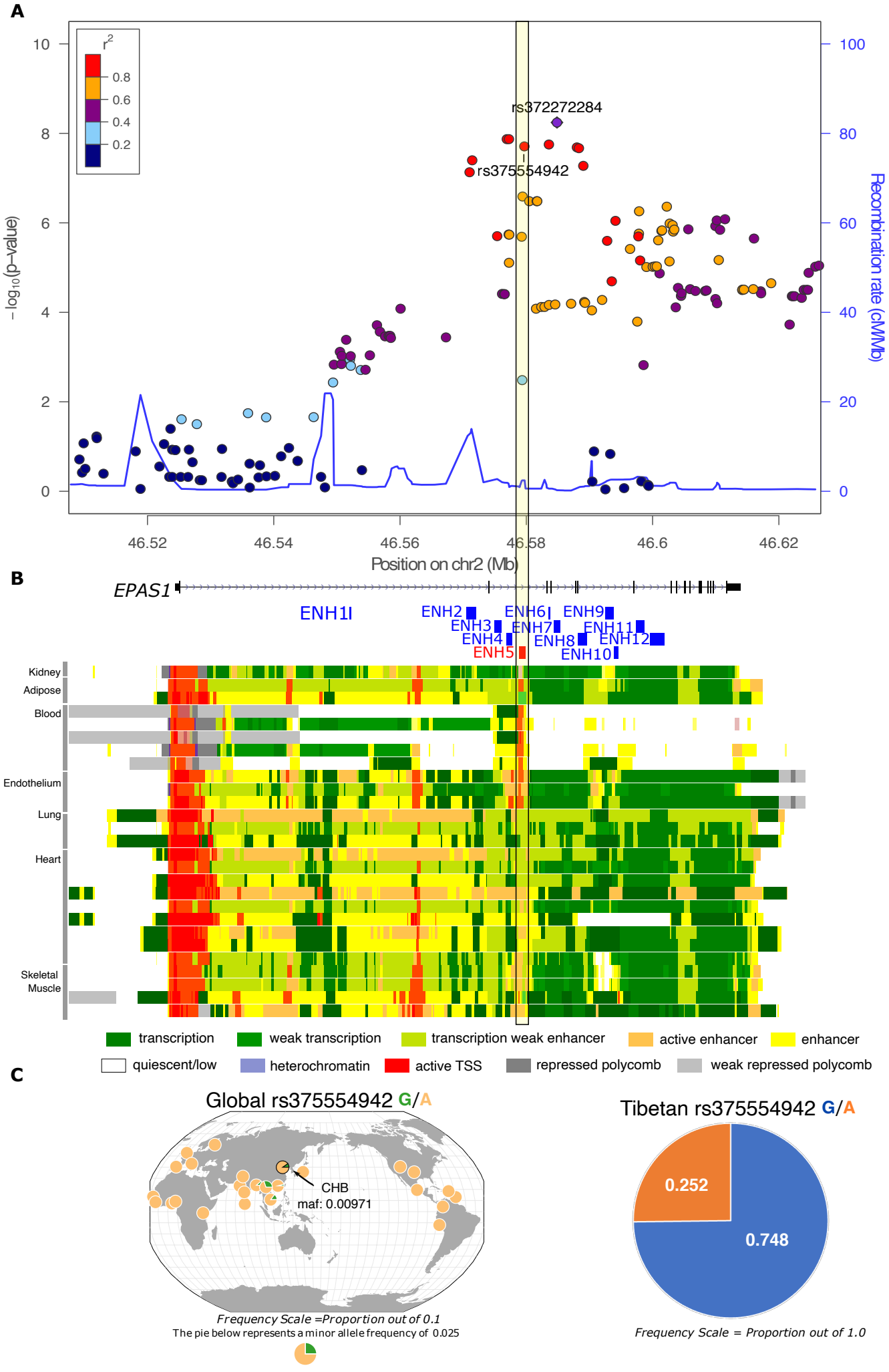
A
r2
0.8
0.6
0.4
0.2
rs372272284
rs375554942
−log10(p−value)
Recombination rate (cM/Mb)
Position on chr2 (Mb)
B
EPAS1
ENH1
ENH2
ENH3
ENH4
ENH5
ENH6
ENH7
ENH8
ENH9
ENH10
ENH11
ENH12
Kidney
Adipose
Blood
Endothelium
Lung
Heart
Skeletal Muscle
transcription
weak transcription
transcription weak enhancer
active enhancer
enhancer
quiescent/low
heterochromatin
active TSS
repressed polycomb
weak repressed polycomb
C
Global rs375554942 G/A
CHB
maf: 0.00971
Frequency Scale =Proportion out of 0.1
The pie below represents a minor allele frequency of 0.025
Tibetan rs375554942 G/A
0.252
0.748
Frequency Scale = Proportion out of 1.0

Fig. S3. Location of luciferase reporter constructs relative to oxygenated hemoglobin association signals and to chromatin states. (A) Locus-zoom plot for the GWAS signal with oxygenated hemoglobin concentration in Tibetans, data from (*17*). (B) Locations of the 12 regions assessed for allelic effects via luciferase reporter assays relative to the predicted chromatin state across multiple tissues. (C) The global and Tibetan allele frequency of rs375554942, the SNP with the top GWAS and selection signal in ENH5. This SNP reached genome-wide significance in a GWAS of Tibetan women for oxygenated Hb concentration (*17*), with the derived G allele being associated with reduced oxygenated hemoglobin concentration among Tibetans.

Site-Directed Mutagenisis ENH5

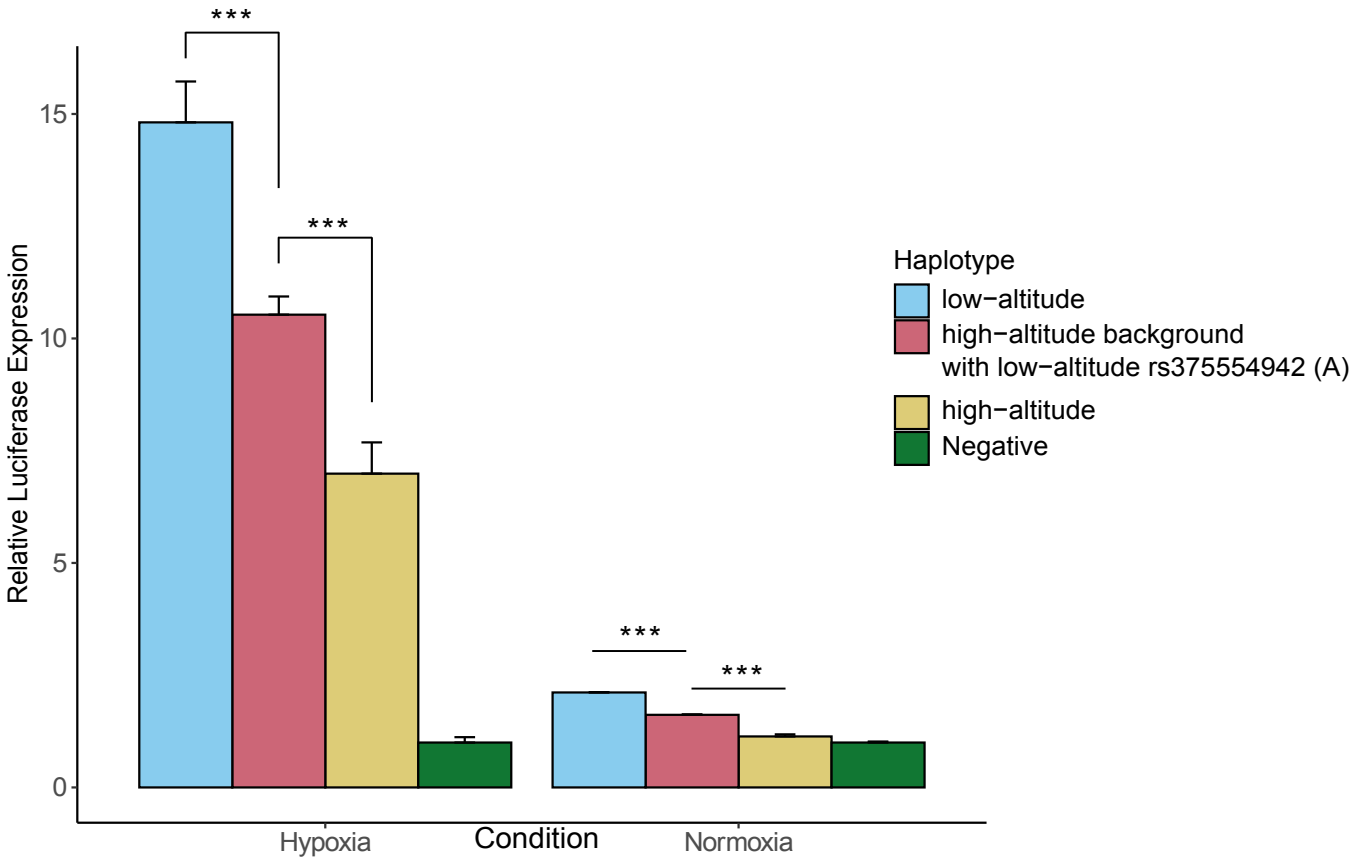

Fig. S4. Relative luciferase expression of mutagenized ENH5. This plot compares the relative luciferase expression of the high and low-altitude alleles of ENH5 to a construct in which one SNP (rs375554942) has been altered by site directed mutagenesis. This construct has a high-altitude haplotype with the low-altitude allele (A) at rs375554842. The results demonstrate that altering this one allele is sufficient to increase the enhancer activity of ENH5.

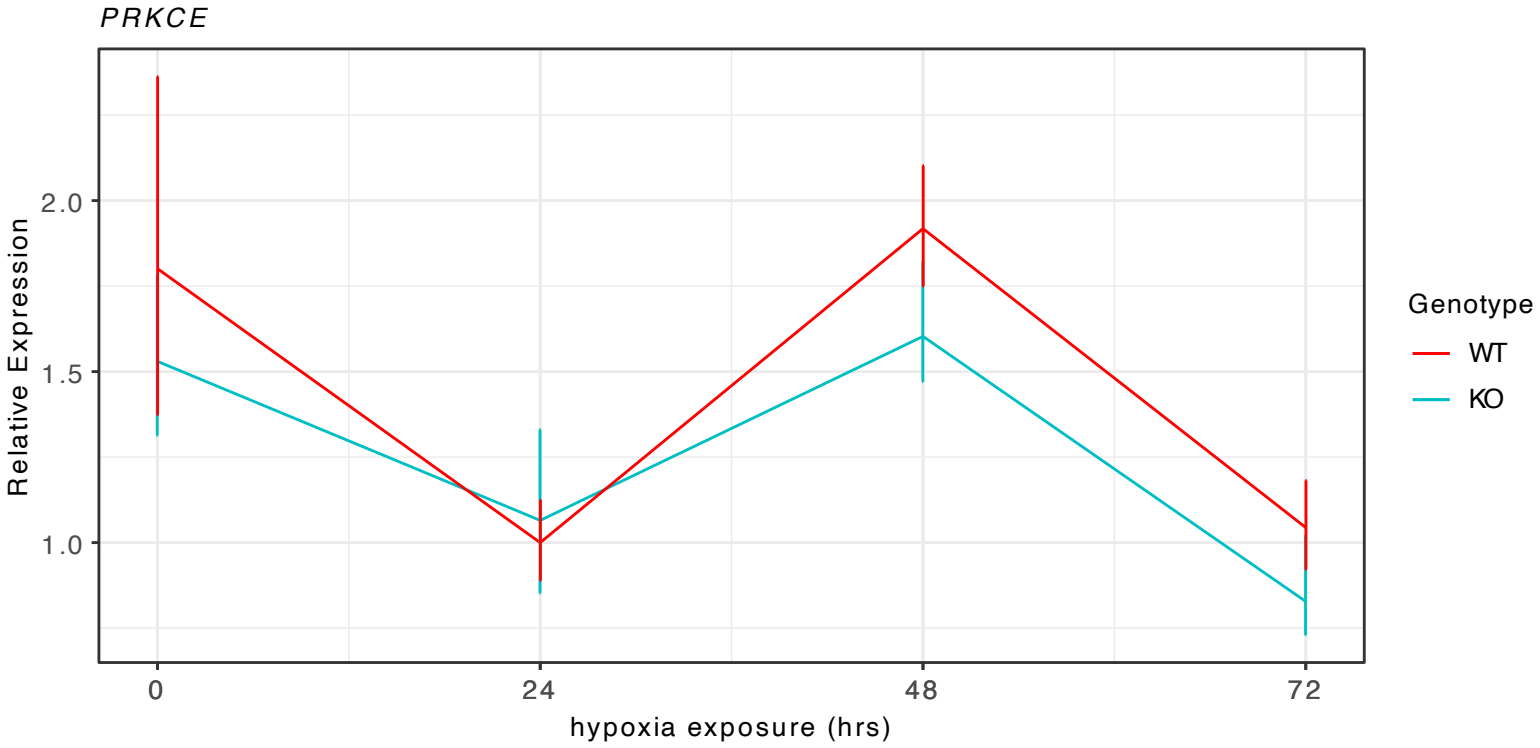
PRKCE
Relative Expression
2.0
1.5
1.0
0
24
48
72
hypoxia exposure (hrs)
Genotype
WT
KO

Fig. S5. Relative *PRKCE* transcript amounts measured by qPCR in the endothelial ENH5 KO clones over a 72-hour hypoxia time course. The red line indicates relative expression of the three homozygous deletion clones, while the blue line indicates the WT controls. Error bars reflect the SEM values for triplicate qPCR reactions performed in each of three clones. No significant differences were observed between WT and KO clones at any hypoxia time point (t-test $P > 0.05$).

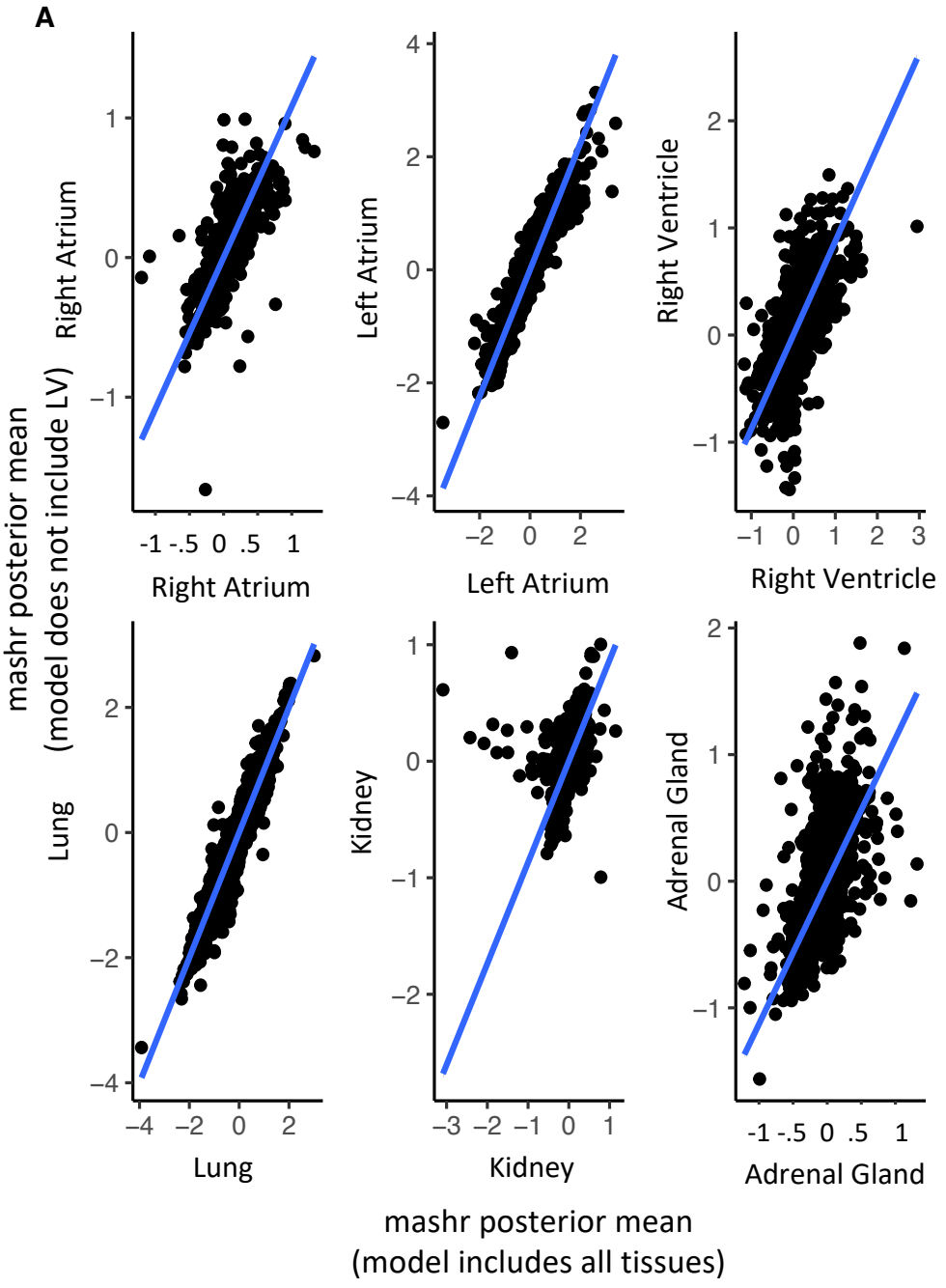
A
mashr posterior mean
(model does not include LV)
Right Atrium
Left Atrium
Right Ventricle
Lung
Kidney
Adrenal Gland
mashr posterior mean
(model includes all tissues)

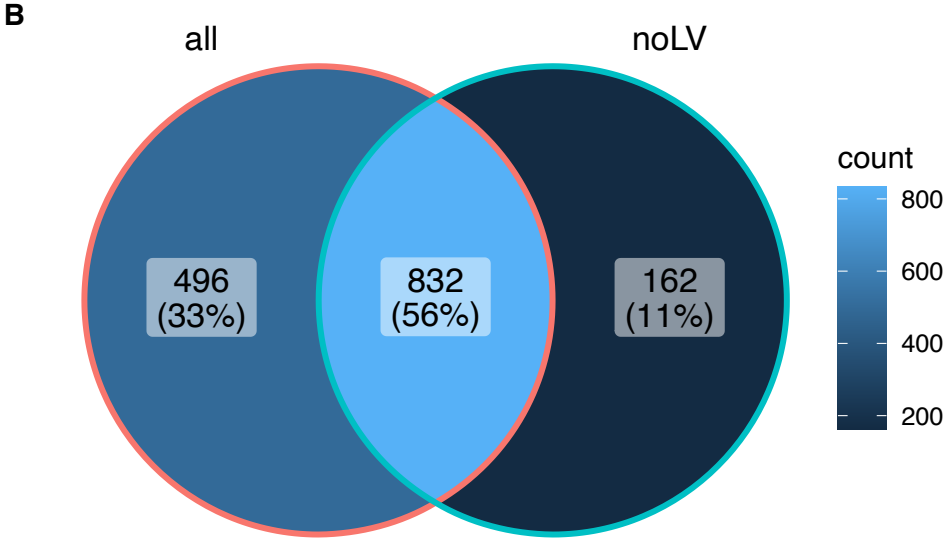
B
all
noLV
count
800
600
400
200
496
(33%)
832
(56%)
162
(11%)

Fig. S6. Inclusion and exclusion of left ventricle from the mashR analysis yield strongly correlated expression patterns. (A) Scatterplot showing the correlation in posterior mean (PM) values of differential expression across genotypes (WT vs. KO) inferred by mashr including all tissues (x-axis) compared to excluding left ventricle (y-axis) for all genes. Strong positive correlation in PM values indicates that inclusion or exclusion of LV does not substantially alter predicted direction of effect for genes in other tissues. For the analyses presented in the main text, we chose to include the LV data. (B) Numbers of significantly DE genes shared between mashr analyses including (all) or excluding (noLV) the left ventricle data. The majority of significantly DE genes are the same across analyses.

Table S1. Differential gene expression and chromatin accessibility in aortic endothelium in response to hypoxia. This Excel file contains results from ATAC-seq and RNA-seq in HAECs exposed to 24 hours of normoxia or hypoxia (1% O_2). First tab shows DE genes identified by DESeq2 in hypoxia vs. normoxia. Second tab shows all peaks identified in normoxia or hypoxia by DiffBind (*78*). The final tab displays all significantly differentially accessible (DA) peaks identified by DiffBind and annotated by Hypergeometric Optimization of Motif EnRichment (HOMER).

Table S2. Candidate SNPs tested in luciferase enhancer assays. This Excel file shows all SNPs contained within the ENH enhancer regions that were tested in luciferase assays. For each SNP we show the rs number, position, *p* values for oxygenated Hb and Hb concentration, PBS score, and PBS *P* value all ascertained in (*17*), as well information on whether the predominant high-altitude allele is shared with Denisovans (*35*).

Table S3. All relative luciferase expression values. This Excel file contains all relative luciferase expression data points calculated for each independent transfection performed. Each tab contains data for a different enhancer region as labeled.

Table S4. Statistical analysis of reporter gene assays in multiple cell types. This Excel file shows *P* values for all comparisons made in reporter gene assays for all luciferase vectors found to have differential enhancer activity between high-altitude and low-altitude alleles. SNPs contained in each validated enhancer region are listed. Results shown represent a minimum of two DNA preparations for each construct with 6 transfection replicates per construct in hypoxia and normoxia. *P* values are from a 1-tailed student's paired t-test between alleles, and a 2-tailed test student's t-test for comparison between normoxia and hypoxia).

Table S5. Positional Weight Matrix (PWM) analysis of all ENH5 candidate SNPs. This Excel file contains the results of HOCOMOCO transcription factor PWM analysis in ENH5. Every other column contains a p value for the indicated mutation combination, the r value is the ratio of the p-value of the mutation over the p-value of the reference sequence for ENH5. The highlighted factors are those for which one or more mutations oblates transcription factor binding which was predicted to be significant in the reference sequence ($p < 1x10^{-04}$). The second tab contains the key for which mutation numbers correspond to which SNP and allele.

Table S6. Statistical analysis of site-directed mutagenesis of ENH5. The results of luciferase assays comparing the enhancer activity of the high-altitude haplotype, low-altitude haplotype, and high-altitude haplotype with rs375554942 mutated to the low altitude ancestral allele (A). *P* values are from a paired 1-tailed student's t tests and represent triplicate transfection replicates per allele and condition.

Region	Condition	p-value high vs low-altitude	p-value high-altitude vs rs375554942 edit	p-value low-altitude vs rs375554942 edit
ENH5	Normoxia	0.0000153	0.0002692	0.0000011
	Hypoxia	0.0012009	0.0058489	0.0063173

Table S7. Summary data from RT-qPCR of CRISPR-modified teloHAECs across hypoxia timepoints. This Excel file shows summary data from qPCR of WT and ENH5 KO teloHAEC lines. Results represent 3 biological replicates per genotype with the value for each clone averaged over 3 qPCR replicates. *P* values were calculated by 1-tailed student's t-test on delta CT values.

Table S8. Blunting of transcriptomic response to chronic hypoxia in CRISPR-modified endothelial cells. This Excel file shows differential expression (Hypoxia – Normoxia) in response to sustained hypoxia (1% O_2, 14 days) assessed by RNA-seq in teloHAEC WT and ENH5 KO clones. Expression was modeled as $\sim \beta_{\text{genotype}} Genotype_i + \beta_{\text{Condition}} Condition_i + \beta_{\text{interaction}} Genotype_i : Condition_i$ and significantly DE genes in response to hypoxia were assessed for each genotype by setting the alternate genotype and normoxia as the baseline in the model. Tabs 1 and 2 show the results of DE analysis for the KO and WT, respectively. These results are polarized as Hypoxia-Normoxia for each. The third tab shows the union of all significantly DE genes detected in the KO and WT along with their respective logFC values, their blunting score (defined in methods), and their interaction term coefficient ($\beta_{\text{interaction}}$).

Table S9. Statistical analysis of mENH5 reporter gene assays. *P* values for testing mENH5 enhancer activity in endothelial, kidney, and cardiac cell lines by luciferase reporter gene assays. Results are for three independent transfection replicates for each of three DNA preparations of the constructs. *P* values are for a paired student's t-test.

Cell type	mENH5 vs negative (normoxia)	mENH5 vs negative (hypoxia)	mENH5 (normoxia) vs mENH5 (hypoxia)
HEK293T	2.89E-08	1.38E-07	4.96E-05
HL-1	3.79E-08	3.89E-10	2.01E-06
teloHAEC	1.82E-05	3.83E-07	0.1898

Table S10. Single-tissue analysis of differential expression between KO and WT mice exposed to hypoxia: This Excel file shows differential expression results for all 7 tissues comparing KO and WT mice after hypoxic exposure. Analyses were performed independently for each tissue using a standard limma-voom pipeline.

Table S11. Results of mashr Analyses of differential gene expression between KO and WT mice exposed to hypoxia. This Excel file shows mashr results for all 7 tissues comparing KO and WT mice after hypoxic exposure. Table shows posterior mean (PM) and local false sign rates (lfsr) for each gene in each tissue.

Table S12. Number and direction of differentially expressed genes identified by mashr (*lfsr* < 0.05) in KO vs WT mice exposed to acute hypoxia using data from 7 tissues

Tissue	Total DE Genes	% Up	% Down
Left Atrium	231	79.2	20.8
Right Atrium	665	50.7	49.3
Left Ventricle	761	83	17
Right Ventricle	369	72.3	27.1
Lung	783	30.7	69.3
Kidney	141	73	27
Adrenal Gland	268	27.6	72.4

Table S13. Selected differentially expressed genes between KO and WT mice exposed to hypoxia. Several genes of interest identified in the mashr analysis as differentially expressed between the mENH5 KO and WT. The sign indicates the direction of effect, significance is calculated by the lfsr statistic and is indicated as follows: * < 0.1, ** < 0.05, *** < 0.01.

	Right Atrium	Left Atrium	Right Ventricle	Left Ventricle	Lung	Kidney	Adrenal Gland	DESCRIPTION
Epas1	NS	- *	NS	NS	- *	NS	NS	Gene target of enhancer mENH5
Cox2	-*	-***	-**	-**	-**	-**	NS	*COX2,* a widely expressed proinflammatory HIF-2α target gene which may impact heart rate, vasoconstriction, and hypertension (49, *52*, *57*)
Id3	+**	+**	+**	NS	+**	+**	+**	*Id3,* a signaling/ proliferation gene known to be inversely regulated by HIF-2α and thought to be involved in the pathogenesis of hypoxia-induced pulmonary hypertension (*21*)
Socs3	+**	+**	+**	NS	+	+*	NS	*Socs3* a potent anti-inflammatory protein which is typically repressed in hypoxia and can inhibit pathogenic angiogenesis in hypoxic conditions (*93*, *94*)
Ddit4	-***	-***	-***	-***	-***	-***	NS	*Ddit4,* or REDD1, a stress response gene known to be activated by HIF-α, which is involved in metabolism, proliferation, and the regulation of apoptosis in response to hypoxia (*95*, *96*).
Dusp5	+**	+**	+**	+**	+**	+**	NS	*Dusp5*, a gene which is suppressed by hypoxia, is a potent vasodilator which acts through suppression the proliferation of smooth muscle cells thereby protecting against pulmonary hypertension (*55*)
Angpt1	-***	-***	-***	-***	NS	NS	NS	*Angpt1* a known endothelial HIF-2α target gene involved in angiogenesis and microvascular maintenance (*48*, *97*)

Table S14. Gene ontology and pathway enrichment analysis for all significantly DE genes from the mashr analysis. Enriched terms of interest are listed.

	Term ID	Term name	Adjusted p value
GO:BP	GO:0009893	positive regulation of metabolic process	1.23E-28
GO:BP	GO:0006950	response to stress	9.56E-22
GO:BP	GO:0072359	circulatory system development	1.10E-20
GO:BP	GO:0001944	vasculature development	2.58E-19
GO:BP	GO:0001525	angiogenesis	6.35E-14
GO:BP	GO:0007155	cell adhesion	3.84E-11
GO:BP	GO:0070482	response to oxygen levels	9.92E-11
GO:BP	GO:0008219	cell death	3.35E-10
GO:BP	GO:0010941	regulation of cell death	6.71E-09
GO:BP	GO:0060048	cardiac muscle contraction	0.000167617
GO:BP	GO:1903522	regulation of blood circulation	0.001031152
KEGG	KEGG:04933	AGE-RAGE signaling pathway in diabetic complications	1.83E-07
KEGG	KEGG:04210	Apoptosis	3.28313E-05
KEGG	KEGG:05200	Pathways in cancer	0.000328847
HP	HP:0011025	Abnormal cardiovascular system physiology	4.08E-08
HP	HP:0031546	Cardiac conduction abnormality	0.000401466
HP	HP:0001297	Stroke	0.000401752
HP	HP:0000822	Hypertension	0.000980866
HP	HP:0002092	Pulmonary arterial hypertension	0.032362484

Table S15. List of CRISPR guides used in human and mouse ENH5 deletion. CRISPR guide sequences used for deleting ENH5 in human teloHAECs and mENH5 in mice along with on- and off-target scores given by IDT's custom guide design tool.

Design ID	Strand	Sequence	PAM	On-Target Score	Off-Target Score	Species	Side
ENH5_L1	+	GTCCTGGAACTTC TCGGAGT	AGG	69	75	*H. sapiens*	Left
ENH5_L2	+	TTCTCGGAGTAGG AAACAAG	AGG	83	50	*H. sapiens*	Left
ENH5_R1	+	GAGGGCAACTAGT TCCACAG	AGG	82	61	*H. sapiens*	Right
ENH5_R2	+	AGGGCAACTAGTT CCACAGA	GGG	86	44	*H. sapiens*	Right
mENH5-L	-	ACGGCAAACATAAA GAGTGT	GGG	77	53	*M. musculus*	Left
mENH5-R	+	GGAAGGGGCCACA CCCAAGC	TGG	71	41	*M. musculus*	Right

Table S16. All primers used in RT-qPCR and genotyping in CRISPR modified cells and mice. Primers used in CRISPR-edited human cell lines and mice. RT-qPCR primers were used to assess expression of genes in endothelial ENH5 KO compared to WT controls. Genotyping primers were used to genotype and identify presence of the desired deletion in both human and mouse deletion lines.

Gene	Left Primer	Right Primer	purpose
h*EPAS1*	CGGAGGTGTTC TATGAGCTGG	AGCTTGTGTG TTCGCAGGAA	RT-qPCR
h*EGLN3*	ATC CGG GAAAT GGAACAGGT	GCAGGATCC CACCATGTAGC	RT-qPCR
h*PRKCE*	CGAGGCCGTGA GCTTGAAG	GCAATGTAGGG GTCGAGAAGG	RT-qPCR
h*RPLP0*	TCAGCAAGTGGGA AGGTGTAATC	TCAGCAAGTGGG AAGGTGTAATC	RT-qPCR
h*EPAS1*	ACC GGGGCT ATTTTTAGCAT	CAG GGT CTCT TCCCTCTGTG	External deletion genotyping primer - used to identify presence of a deletion band or WT band.
h*EPAS1*	GAGCCATCTCT CGTCTTTGG	TAAGGTGATGCC ACAATCCA	Internal deletion genotyping primer – Used to identify presence or absence sequence within the ENH5 enhancer.
m*EPAS1*	ACTGACTGTA GCGCCCCATA	GTCCAGCACG CT TACTTCCA	External deletion genotyping primer – used to identify presence of a deletion band or WT band.
m*EPAS1*	CTGCCACCTG CTAGTTCACA	CTACATCCTG GCCATTTGCT	Internal deletion genotyping primer - Used to identify presence or absence sequence within the mENH5 enhancer.

Data file S1. HiCUP Processing report (separate file in PDF format). This file contains QC information pertaining to the analysis of Capture Hi-C data and is automatically generated by the HiCUP processing pipeline (*98*). This report indicates the overall good quality of the capture Hi-C analysis performed in HAEC

REFERENCES AND NOTES

1. S. Fan, M. E. B. Hansen, Y. Lo, S. A. Tishkoff, Going global by adapting local: A review of recent human adaptation. *Science* **354**, 54–59 (2016).

2. G. Coop, J. K. Pickrell, J. Novembre, S. Kudaravalli, J. Li, D. Absher, R. M. Myers, L. L. Cavalli-Sforza, M. W. Feldman, J. K. Pritchard, The role of geography in human adaptation. *PLOS Genet.* **5**, e1000500 (2009).

3. R. D. Hernandez, J. L. Kelley, E. Elyashiv, S. C. Melton, A. Auton, G. McVean; 1000 Genomes Project, G. Sella, M. Przeworski, Classic selective sweeps were rare in recent human evolution. *Science* **331**, 920–924 (2011).

4. D. Murphy, E. Elyashiv, G. Amster, G. Sella, "Broad-scale variation in human genetic diversity levels is predicted by purifying selection on coding and non-coding elements". *bioRxiv* 2021.07.02.450762 (2021).

5. Y. G. Kamberov, S. Wang, J. Tan, P. Gerbault, A. Wark, L. Tan, Y. Yang, S. Li, K. Tang, H. Chen, A. Powell, Y. Itan, D. Fuller, J. Lohmueller, J. Mao, A. Schachar, M. Paymer, E. Hostetter, E. Byrne, M. Burnett, A. P. McMahon, M. G. Thomas, D. E. Lieberman, L. Jin, C. J. Tabin, B. A. Morgan, P. C. Sabeti, Modeling recent human evolution in mice by expression of a selected EDAR variant. *Cell* **152**, 691–702 (2013).

6. C. M. Beall, Natural selection on EPAS1 (HIF2alpha) associated with low hemoglobin concentration in Tibetan highlanders. *Proc. Natl. Acad. Sci. U.S.A.* **107**, 11459–11464 (2010).

7. T. S. Simonson, Y. Yang, C. D. Huff, H. Yun, G. Qin, D. J. Witherspoon, Z. Bai, F. R. Lorenzo, J. Xing, L. B. Jorde, J. T. Prchal, R. Ge, Genetic evidence for high-altitude adaptation in Tibet. *Science* **329**, 72–75 (2010).

8. X. Yi, Y. Liang, E. Huerta-Sanchez, X. Jin, Z. X. P. Cuo, J. E. Pool, X. Xu, H. Jiang, N. Vinckenbosch, T. S. Korneliussen, H. Zheng, T. Liu, W. He, K. Li, R. Luo, X. Nie, H. Wu, M. Zhao, H. Cao, J. Zou, Y. Shan, S. Li, Q. Yang, Asan, P. Ni, G. Tian, J. Xu, X. Liu, T. Jiang, R. Wu, G. Zhou, M. Tang, J. Qin, T. Wang, S. Feng, G. Li, Huasang, J. Luosang, W. Wang, F. Chen, Y. Wang, X. Zheng, Z. Li, Z. Bianba,

G. Yang, X. Wang, S. Tang, G. Gao, Y. Chen, Z. Luo, L. Gusang, Z. Cao, Q. Zhang, W. Ouyang, X. Ren, H. Liang, H. Zheng, Y. Huang, J. Li, L. Bolund, K. Kristiansen, Y. Li, Y. Zhang, X. Zhang, R. Li, S. Li, H. Yang, R. Nielsen, J. Wang, J. Wang, Sequencing of 50 human exomes reveals adaptation to high altitude. *Science* **329**, 75–78 (2010).

9. J. A. Horscroft, A. O. Kotwica, V. Laner, J. A. West, P. J. Hennis, D. Z. H. Levett, D. J. Howard, B. O. Fernandez, S. L. Burgess, Z. Ament, E. T. Gilbert-Kawai, A. Vercueil, B. D. Landis, K. Mitchell, M. G. Mythen, C. Branco, R. S. Johnson, M. Feelisch, H. E. Montgomery, J. L. Griffin, M. P. W. Grocott, E. Gnaiger, D. S. Martin, A. J. Murray, Metabolic basis to Sherpa altitude adaptation. *Proc. Natl. Acad. Sci. U.S.A.* **114**, 6382–6387 (2017).

10. S. Miller, C. Tudor, V. Thorsten, U. U. Nyima, U. Sonam, U. Droyoung, L. Wright, M. Varner, Comparison of maternal and newborn outcomes of Tibetan and Han Chinese delivering in Lhasa, Tibet. *J. Obstet. Gynaecol. Res.* **34**, 986–993 (2008).

11. S. F. Sun, T. S. Droma, J. G. Zhang, J. X. Tao, S. Y. Huang, R. G. McCullough, R. E. McCullough, C. S. Reeves, J. T. Reeves, L. G. Moore, Greater maximal O_2 uptakes and vital capacities in Tibetan than Han residents of Lhasa. *Respir. Physiol.* **79**, 151–161 (1990).

12. C. M. Beall, Two routes to functional adaptation: Tibetan and Andean high-altitude natives. *Proc. Natl. Acad. Sci. U.S.A.* **104**, 8655–8660 (2007).

13. A. W. Bigham, F. S. Lee, Human high-altitude adaptation: Forward genetics meets the HIF pathway. *Genes Dev.* **28**, 2189–2204 (2014).

14. L. G. Moore, D. Young, R. E. McCullough, T. Droma, S. Zamudio, Tibetan protection from intrauterine growth restriction (IUGR) and reproductive loss at high altitude. *Am. J. Hum. Biol.* **13**, 635–644 (2001).

15. B. M. Groves, T. Droma, J. R. Sutton, R. G. McCullough, R. E. McCullough, J. Zhuang, G. Rapmund, S. Sun, C. Janes, L. G. Moore, Minimal hypoxic pulmonary hypertension in normal Tibetans at 3,658 m. *J. Appl. Physiol. (1985)* **74**, 312–318 (1993).

16. N. Petousi, Q. P. P. Croft, G. L. Cavalleri, H.-Y. Cheng, F. Formenti, K. Ishida, D. Lunn, M. McCormack, K. V. Shianna, N. P. Talbot, P. J. Ratcliffe, P. A. Robbins, Tibetans living at sea level have a hyporesponsive hypoxia-inducible factor system and blunted physiological responses to hypoxia. *J. Appl. Physiol. (1985)* **116**, 893–904 (2014).

17. C. Jeong, D. B. Witonsky, B. Basnyat, M. Neupane, C. M. Beall, G. Childs, S. R. Craig, J. Novembre, A. D. Rienzo, Detecting past and ongoing natural selection among ethnically Tibetan women at high altitude in Nepal. *PLOS Genet.* **14**, e1007650 (2018).

18. C. M. Beall, Quantitative genetic analysis of arterial oxygen saturation in Tibetan highlanders. *Hum. Biol.* **69**, 597–604 (1997).

19. Y. Peng, C. Cui, Y. He, Ouzhuluobu, H. Zhang, D. Yang, Q. Zhang, Bianbazhuoma, L. Yang, Y. He, K. Xiang, X. Zhang, S. Bhandari, P. Shi, Yangla, Dejiquzong, Baimakangzhuo, Duojizhuoma, Y. Pan, Cirenyangji, Baimayangji, Gonggalanzi, C. Bai, Bianba, Basang, Ciwangsangbu, S. Xu, H. Chen, S. Liu, T. Wu, X. Qi, B. Su, Down-regulation of EPAS1 transcription and genetic adaptation of tibetans to high-altitude hypoxia. *Mol. Biol. Evol.* **34**, 818–830 (2017).

20. C. E. Green, A. M. Turner, The role of the endothelium in asthma and chronic obstructive pulmonary disease (COPD). *Respir. Res.* **18**, 20 (2017).

21. C.-J. Hu, J. M. Poth, H. Zhang, A. Flockton, A. Laux, S. Kumar, B. McKeon, G. Mouradian, M. Li, S. Riddle, S. C. Pugliese, R. D. Brown, E. M. Wallace, B. B. Graham, M. G. Frid, K. R. Stenmark, Suppression of HIF2 signalling attenuates the initiation of hypoxia-induced pulmonary hypertension. *Eur. Respir. J.* **54**, 1900378 (2019).

22. R. Bartoszewski, A. Moszyńska, M. Serocki, A. Cabaj, A. Polten, R. Ochocka, L. Dell'Italia, S. Bartoszewska, J. Króliczewski, M. Dąbrowski, J. F. Collawn, Primary endothelial cell–Specific regulation of hypoxia-inducible factor (HIF)-1 and HIF-2 and their target gene expression profiles during hypoxia. *FASEB J.* **33**, 7929–7941 (2019).

23. B. L. Krock, N. Skuli, M. C. Simon, Hypoxia-induced angiogenesis: Good and evil. *Genes Cancer* **2**, 1117–1133 (2011).

24. P. I. Aaronson, T. P. Robertson, G. A. Knock, S. Becker, T. H. Lewis, V. Snetkov, J. P. T. Ward, Hypoxic pulmonary vasoconstriction: Mechanisms and controversies. *J. Physiol.* **570**, 53–58 (2006).

25. L. Claesson-Welsh, E. Dejana, D. M. McDonald, Permeability of the endothelial barrier: Identifying and reconciling controversies. *Trends Mol. Med.* **27**, 314–331 (2021).

26. M. Batie, L. del Peso, S. Rocha, Hypoxia and chromatin: A focus on transcriptional repression mechanisms. *Biomedicine* **6**, 47 (2018).

27. A. B. Johnson, M. C. Barton, Hypoxia-induced and stress-specific changes in chromatin structure and function. *Mutat. Res.* **618**, 149–162 (2007).

28. I. Jung, A. Schmitt, Y. Diao, A. J. Lee, T. Liu, D. Yang, C. Tan, J. Eom, M. Chan, S. Chee, Z. Chiang, C. Kim, E. Masliah, C. L. Barr, B. Li, S. Kuan, D. Kim, B. Ren, A compendium of promoter-centered long-range chromatin interactions in the human genome. *Nat. Genet.* **51**, 1442–1449 (2019).

29. J. Li, J. T. Glessner, H. Zhang, C. Hou, Z. Wei, J. P. Bradfield, F. D. Mentch, Y. Guo, C. Kim, Q. Xia, R. M. Chiavacci, K. A. Thomas, H. Qiu, S. F. A. Grant, S. L. Furth, H. Hakonarson, P. M. A. Sleiman, GWAS of blood cell traits identifies novel associated loci and epistatic interactions in Caucasian and African-American children. *Hum. Mol. Genet.* **22**, 1457–1464 (2013).

30. A. Buniello, J. A. L. MacArthur, M. Cerezo, L. W. Harris, J. Hayhurst, C. Malangone, A. McMahon, J. Morales, E. Mountjoy, E. Sollis, D. Suveges, O. Vrousgou, P. L. Whetzel, R. Amode, J. A. Guillen, H. S. Riat, S. J. Trevanion, P. Hall, H. Junkins, P. Flicek, T. Burdett, L. A. Hindorff, F. Cunningham, H. Parkinson, The NHGRI-EBI GWAS catalog of published genome-wide association studies, targeted arrays and summary statistics 2019. *Nucleic Acids Res.* **47**, D1005–D1012 (2019).

31. Y. Wang, F. Song, B. Zhang, L. Zhang, J. Xu, D. Kuang, D. Li, M. N. K. Choudhary, Y. Li, M. Hu, R. Hardison, T. Wang, F. Yue, The 3D genome browser: A web-based browser for visualizing 3D genome organization and long-range chromatin interactions. *Genome Biol.* **19**, 151 (2018).

32. L. E. Montefiori, D. R. Sobreira, N. J. Sakabe, I. Aneas, A. C. Joslin, G. T. Hansen, G. Bozek, I. P. Moskowitz, E. M. McNally, M. A. Nóbrega, A promoter interaction map for cardiovascular disease genetics. *eLife* **7**, e35788 (2018).

33. D. R. Sobreira, A. C. Joslin, Q. Zhang, I. Williamson, G. T. Hansen, K. M. Farris, N. J. Sakabe, N. Sinnott-Armstrong, G. Bozek, S. O. Jensen-Cody, K. H. Flippo, C. Ober, W. A. Bickmore, M. Potthoff, M. Chen, M. Claussnitzer, I. Aneas, M. A. Nóbrega, Extensive pleiotropism and allelic heterogeneity mediate metabolic effects of *IRX3* and *IRX5*. *Science* **372**, 1085–1091 (2021).

34. B. Mifsud, F. Tavares-Cadete, A. N. Young, R. Sugar, S. Schoenfelder, L. Ferreira, S. W. Wingett, S. Andrews, W. Grey, P. A. Ewels, B. Herman, S. Happe, A. Higgs, E. LeProust, G. A. Follows, P. Fraser, N. M. Luscombe, C. S. Osborne, Mapping long-range promoter contacts in human cells with high-resolution capture Hi-C. *Nat. Genet.* **47**, 598–606 (2015).

35. E. Huerta-Sánchez, X. Jin, Asan, Z. Bianba, B. M. Peter, N. Vinckenbosch, Y. Liang, X. Yi, M. He, M. Somel, P. Ni, B. Wang, X. Ou, Huasang, J. Luosang, Z. X. P. Cuo, K. Li, G. Gao, Y. Yin, W. Wang, X. Zhang, X. Xu, H. Yang, Y. Li, R. Nielsen, Altitude adaptation in Tibetans caused by introgression of Denisovan-like DNA. *Nature* **512**, 194–197 (2014).

36. M. J. Percy, P. W. Furlow, G. S. Lucas, X. Li, T. R. J. Lappin, M. F. McMullin, F. S. Lee, A gain-of-function mutation in the HIF2A gene in familial erythrocytosis. *N. Engl. J. Med.* **358**, 162–168 (2008).

37. N. L. Downes, N. Laham-Karam, M. U. Kaikkonen, S. Ylä-Herttuala, Differential but complementary HIF1α and HIF2α transcriptional regulation. *Mol. Ther.* **26**, 1735–1745 (2018).

38. W. J. Kent, C. W. Sugnet, T. S. Furey, K. M. Roskin, T. H. Pringle, A. M. Zahler, D. Haussler, The human genome browser at UCSC. *Genome Res.* **12**, 996–1006 (2002).

39. J. Ernst, M. Kellis, ChromHMM: Automating chromatin-state discovery and characterization. *Nat. Methods* **9**, 215–216 (2012).

40. X. Zhou, D. Li, B. Zhang, R. F. Lowdon, N. B. Rockweiler, R. L. Sears, P. A. F. Madden, I. Smirnov, J. F. Costello, T. Wang, Epigenomic annotation of genetic variants using the roadmap epigenome browser. *Nat. Biotechnol.* **33**, 345–346 (2015).

41. A. C. Joslin, D. R. Sobreira, G. T. Hansen, N. J. Sakabe, I. Aneas, L. E. Montefiori, K. M. Farris, J. Gu, D. M. Lehman, C. Ober, X. He, M. A. Nóbrega, A functional genomics pipeline identifies

pleiotropy and cross-tissue effects within obesity-associated GWAS loci. *Nat. Commun.* **12**, 5253 (2021).

42. M. C. Simon, L. Liu, B. C. Barnhart, R. M. Young, Hypoxia-induced signaling in the cardiovascular system. *Annu. Rev. Physiol.* **70**, 51–71 (2008).

43. R. Naeije, Physiological adaptation of the cardiovascular system to high altitude. *Prog. Cardiovasc. Dis.* **52**, 456–466 (2010).

44. L. Bernardi, "Heart Rate and Cardiovascular Variability at High Altitude" in *2007 29th Annual International Conference of the IEEE Engineering in Medicine and Biology Society* (IEEE, Lyon, France, 2007; http://ieeexplore.ieee.org/document/4353892/), pp. 6678–6680.

45. F. León-Velarde, F. C. Villafuerte, J.-P. Richalet, Chronic mountain sickness and the heart. *Prog. Cardiovasc. Dis.* **52**, 540–549 (2010).

46. J. E. Crawford, R. Amaru, J. Song, C. G. Julian, F. Racimo, J. Y. Cheng, X. Guo, J. Yao, B. Ambale-Venkatesh, J. A. Lima, J. I. Rotter, J. Stehlik, L. G. Moore, J. T. Prchal, R. Nielsen, Natural selection on genes related to cardiovascular health in high-altitude adapted andeans. *Am. J. Hum. Genet.* **101**, 752–767 (2017).

47. X. Li, Z.-N. Han, Y. Liu, L. Hong, B.-R. Cui, X. Cui, Endogenous ET-1 promotes ANP secretion through activation of COX2-L-PGDS-PPARγ signaling in hypoxic beating rat atria. *Peptides* **122**, 170150 (2019).

48. V. L. Dengler, M. Galbraith, J. M. Espinosa, Transcriptional regulation by hypoxia inducible factors. *Crit. Rev. Biochem. Mol. Biol.* **49**, 1–15 (2014).

49. X. Xue, Y. M. Shah, Hypoxia-inducible factor-2α is essential in activating the COX2/mPGES-1/PGE_2 signaling axis in colon cancer. *Carcinogenesis* **34**, 163–169 (2013).

50. S. M. Urbut, G. Wang, P. Carbonetto, M. Stephens, Flexible statistical methods for estimating and testing effects in genomic studies with multiple conditions. *Nat. Genet.* **51**, 187–195 (2019).

51. O. A. Gray, J. Yoo, D. R. Sobreira, J. Jousma, D. Witonsky, Y.-J. Peng, N. R. Prabhakar, Y. Fang, M. A. Nóbrega, "Supplementary Materials for: A pleiotropic hypoxia-sensitive EPAS1 enhancer is disrupted by adaptive alleles in Tibetans."

52. X. Yang, K. K. K. Sheares, N. Davie, P. D. Upton, G. W. Taylor, J. Horsley, J. Wharton, N. W. Morrell, Hypoxic induction of Cox-2 regulates proliferation of human pulmonary artery smooth muscle cells. *Am. J. Respir. Cell Mol. Biol.* **27**, 688–696 (2002).

53. Y.-T. Chang, C.-N. Tseng, P. Tannenberg, L. Eriksson, K. Yuan, V. A. de Jesus Perez, J. Lundberg, M. Lengquist, I. R. Botusan, S.-B. Catrina, P.-K. Tran, U. Hedin, K. Tran-Lundmark, Perlecan heparan sulfate deficiency impairs pulmonary vascular development and attenuates hypoxic pulmonary hypertension. *Cardiovasc. Res.* **107**, 20–31 (2015).

54. L. Bai, Z. Yu, G. Qian, P. Qian, J. Jiang, G. Wang, C. Bai, SOCS3 was induced by hypoxia and suppressed STAT3 phosphorylation in pulmonary arterial smooth muscle cells. *Respir. Physiol. Neurobiol.* **152**, 83–91 (2006).

55. B. S. Ferguson, S. A. Wennersten, K. M. Demos-Davies, M. Rubino, E. L. Robinson, M. A. Cavasin, M. S. Stratton, A. M. Kidger, T. Hu, S. M. Keyse, R. A. McKnight, R. H. Lane, E. S. Nozik, M. C. M. Weiser-Evans, T. A. McKinsey, DUSP5-mediated inhibition of smooth muscle cell proliferation suppresses pulmonary hypertension and right ventricular hypertrophy. *Am. J. Physiol. Heart Circ. Physiol.* **321**, H382–H389 (2021).

56. J. Xin, H. Zhang, Y. He, Z. Duren, C. Bai, L. Chen, X. Luo, D.-S. Yan, C. Zhang, X. Zhu, Q. Yuan, Z. Feng, C. Cui, X. Qi, Ouzhuluobu, W. H. Wong, Y. Wang, B. Su, Chromatin accessibility landscape and regulatory network of high-altitude hypoxia adaptation. *Nat. Commun.* **11**, 4928 (2020).

57. J. Quilley, Y.-J. Chen, Role of COX-2 in the enhanced vasoconstrictor effect of arachidonic acid in the diabetic rat kidney. *Hypertension* **42**, 837–843 (2003).

58. S. A. Watson, G. P. McStay, Functions of cytochrome c oxidase assembly factors. *Int. J. Mol. Sci.* **21**, E7254 (2020).

59. S. L. Archambeault, L. R. Bärtschi, A. D. Merminod, C. L. Peichel, Adaptation via pleiotropy and linkage: Association mapping reveals a complex genetic architecture within the stickleback *Eda* locus. *Evol. Lett.* **4**, 282–301 (2020).

60. J. K. Pritchard, A. Di Rienzo, Adaptation – Not by sweeps alone. *Nat. Rev. Genet.* **11**, 665–667 (2010).

61. K. Watanabe, S. Stringer, O. Frei, M. Umićević Mirkov, C. de Leeuw, T. J. C. Polderman, S. van der Sluis, O. A. Andreassen, B. M. Neale, D. Posthuma, A global overview of pleiotropy and genetic architecture in complex traits. *Nat. Genet.* **51**, 1339–1348 (2019).

62. S. B. Carroll, Evo-devo and an expanding evolutionary synthesis: A genetic theory of morphological evolution. *Cell* **134**, 25–36 (2008).

63. GTEx Consortium, The GTEx consortium atlas of genetic regulatory effects across human tissues. *Science* **369**, 1318–1330 (2020).

64. T. D. Price, A. Qvarnström, D. E. Irwin, The role of phenotypic plasticity in driving genetic evolution. *Proc. R. Soc. Lond. B Biol. Sci.* **270**, 1433–1440 (2003).

65. J. F. Storz, G. R. Scott, Z. A. Cheviron, Phenotypic plasticity and genetic adaptation to high-altitude hypoxia in vertebrates. *J. Exp. Biol.* **213**, 4125–4136 (2010).

66. J. Merilä, Perplexing effects of phenotypic plasticity. *Nature* **525**, 326–327 (2015).

67. C. K. Ghalambor, J. K. McKAY, S. P. Carroll, D. N. Reznick, Adaptive versus non-adaptive phenotypic plasticity and the potential for contemporary adaptation in new environments. *Funct. Ecol.* **21**, 394–407 (2007).

68. D. Song, A. W. Bigham, F. S. Lee, High-altitude deer mouse hypoxia-inducible factor-2α shows defective interaction with CREB-binding protein. *J. Biol. Chem.* **296**, 100461 (2021).

69. C. M. Ivy, J. P. Velotta, Z. A. Cheviron, G. R. Scott, Genetic variation in HIF-2α attenuates ventilatory sensitivity and carotid body growth in chronic hypoxia in high-altitude deer mice. *J. Physiol.* **600**, 4207–4225 (2022).

70. C. L. Peichel, D. A. Marques, The genetic and molecular architecture of phenotypic diversity in sticklebacks. *Philos. Trans. R. Soc. B Biol. Sci.* **372**, 20150486 (2017).

71. D. J. Green, J. H. Walsh, A. Maiorana, V. Burke, R. R. Taylor, J. G. O'Driscoll, Comparison of resistance and conduit vessel nitric oxide-mediated vascular function in vivo: Effects of exercise training. *J. Appl. Physiol. (1985)* **97**, 749–755 (2004).

72. J. D. Buenrostro, B. Wu, H. Y. Chang, W. J. Greenleaf, ATAC-seq: A method for assaying chromatin accessibility genome-wide. *Curr. Protoc. Mol. Biol.* **109**, 21.29.1–21.29.9 (2015).

73. A. Dobin, C. A. Davis, F. Schlesinger, J. Drenkow, C. Zaleski, S. Jha, P. Batut, M. Chaisson, T. R. Gingeras, STAR: Ultrafast universal RNA-seq aligner. *Bioinforma. Oxf. Engl.* **29**, 15–21 (2013).

74. B. Li, C. N. Dewey, RSEM: Accurate transcript quantification from RNA-seq data with or without a reference genome. *BMC Bioinformatics* **12**, 323 (2011).

75. Sequence Alignment/Map format and SAMtools | Bioinformatics | Oxford Academic, (https://academic.oup.com/bioinformatics/article/25/16/2078/204688).

76. Y. Zhang, T. Liu, C. A. Meyer, J. Eeckhoute, D. S. Johnson, B. E. Bernstein, C. Nusbaum, R. M. Myers, M. Brown, W. Li, X. S. Liu, Model-based analysis of ChIP-Seq (MACS). *Genome Biol.* **9**, R137 (2008).

77. C. S. Ross-Innes, R. Stark, A. E. Teschendorff, K. A. Holmes, H. R. Ali, M. J. Dunning, G. D. Brown, O. Gojis, I. O. Ellis, A. R. Green, S. Ali, S.-F. Chin, C. Palmieri, C. Caldas, J. S. Carroll, Differential oestrogen receptor binding is associated with clinical outcome in breast cancer. *Nature* **481**, 389–393 (2012).

78. S. S. P. Rao, M. H. Huntley, N. C. Durand, E. K. Stamenova, I. D. Bochkov, J. T. Robinson, A. L. Sanborn, I. Machol, A. D. Omer, E. S. Lander, E. L. Aiden, A 3D map of the human genome at kilobase resolution reveals principles of chromatin looping. *Cell* **159**, 1665–1680 (2014).

79. S. Heinz, C. Benner, N. Spann, E. Bertolino, Y. C. Lin, P. Laslo, J. X. Cheng, C. Murre, H. Singh, C. K. Glass, Simple combinations of lineage-determining transcription factors prime cis-regulatory elements required for macrophage and B cell identities. *Mol. Cell* **38**, 576–589 (2010).

80. W. C. Claycomb, N. A. Lanson Jr., B. S. Stallworth, D. B. Egeland, J. B. Delcarpio, A. Bahinski, N. J. Izzo, HL-1 cells: A cardiac muscle cell line that contracts and retains phenotypic characteristics of the adult cardiomyocyte. *Proc. Natl. Acad. Sci. U.S.A.* **95**, 2979–2984 (1998).

81. I. V. Kulakovskiy, I. E. Vorontsov, I. S. Yevshin, R. N. Sharipov, A. D. Fedorova, E. I. Rumynskiy, Y. A. Medvedeva, A. Magana-Mora, V. B. Bajic, D. A. Papatsenko, F. A. Kolpakov, V. J. Makeev, HOCOMOCO: Towards a complete collection of transcription factor binding models for human and mouse via large-scale ChIP-seq analysis. *Nucleic Acids Res.* **46**, D252–D259 (2018).

82. M. D. Krause, R.-T. Huang, D. Wu, T.-P. Shentu, D. L. Harrison, M. B. Whalen, L. K. Stolze, A. Di Rienzo, I. P. Moskowitz, M. Civelek, C. E. Romanoski, Y. Fang, Genetic variant at coronary artery disease and ischemic stroke locus 1p32.2 regulates endothelial responses to hemodynamics. *Proc. Natl. Acad. Sci. U.S.A.* **115**, E11349–E11358 (2018).

83. S. Bakhashab, S. Lary, F. Ahmed, H.-J. Schulten, A. Bashir, F. W. Ahmed, A. L. Al-Malki, H. S. Jamal, M. A. Gari, J. U. Weaver, Reference genes for expression studies in hypoxia and hyperglycemia models in human umbilical vein endothelial cells. *G3 (Bethesda)* **4**, 2159–2165 (2014).

84. B. Phipson, S. Lee, I. J. Majewski, W. S. Alexander, G. K. Smyth, Robust hyperparameter estimation protects against hypervariable genes and improves power to detect differential expression. *Ann. Appl. Stat.* **10**, 946–963 (2016).

85. C. W. Law, Y. Chen, W. Shi, G. K. Smyth, voom: Precision weights unlock linear model analysis tools for RNA-seq read counts. *Genome Biol.* **15**, R29 (2014).

86. B. Wang, Y.-J. Peng, X. Su, C. Zhang, J. S. Nagati, J. A. Garcia, N. R. Prabhakar, Olfactory receptor 78 regulates erythropoietin and cardiorespiratory responses to hypobaric hypoxia. *J. Appl. Physiol. (1985)* **130**, 1122–1132 (2021).

87. D. D. Kline, T. Yang, P. L. Huang, N. R. Prabhakar, Altered respiratory responses to hypoxia in mutant mice deficient in neuronal nitric oxide synthase. *J. Physiol.* **511**, 273–287 (1998).

88. U. Raudvere, L. Kolberg, I. Kuzmin, T. Arak, P. Adler, H. Peterson, J. Vilo, g:Profiler: A web server for functional enrichment analysis and conversions of gene lists (2019 update). *Nucleic Acids Res.* **47**, W191–W198 (2019).

89. F. Cunningham, P. Achuthan, W. Akanni, J. Allen, M. R. Amode, I. M. Armean, R. Bennett, J. Bhai, K. Billis, S. Boddu, C. Cummins, C. Davidson, K. J. Dodiya, A. Gall, C. G. Girón, L. Gil, T. Grego, L. Haggerty, E. Haskell, T. Hourlier, O. G. Izuogu, S. H. Janacek, T. Juettemann, M. Kay, M. R. Laird, I. Lavidas, Z. Liu, J. E. Loveland, J. C. Marugán, T. Maurel, A. C. McMahon, B. Moore, J. Morales, J. M. Mudge, M. Nuhn, D. Ogeh, A. Parker, A. Parton, M. Patricio, A. I. Abdul Salam, B. M. Schmitt, H. Schuilenburg, D. Sheppard, H. Sparrow, E. Stapleton, M. Szuba, K. Taylor, G. Threadgold, A. Thormann, A. Vullo, B. Walts, A. Winterbottom, A. Zadissa, M. Chakiachvili, A. Frankish, S. E. Hunt, M. Kostadima, N. Langridge, F. J. Martin, M. Muffato, E. Perry, M. Ruffier, D. M. Staines, S. J. Trevanion, B. L. Aken, A. D. Yates, D. R. Zerbino, P. Flicek, Ensembl 2019. *Nucleic Acids Res.* **47**, D745–D751 (2019).

90. M. Kanehisa, Y. Sato, M. Furumichi, K. Morishima, M. Tanabe, New approach for understanding genome variations in KEGG. *Nucleic Acids Res.* **47**, D590–D595 (2019).

91. D. N. Slenter, M. Kutmon, K. Hanspers, A. Riutta, J. Windsor, N. Nunes, J. Mélius, E. Cirillo, S. L. Coort, D. Digles, F. Ehrhart, P. Giesbertz, M. Kalafati, M. Martens, R. Miller, K. Nishida, L. Rieswijk, A. Waagmeester, L. M. T. Eijssen, C. T. Evelo, A. R. Pico, E. L. Willighagen, WikiPathways: A multifaceted pathway database bridging metabolomics to other omics research. *Nucleic Acids Res.* **46**, D661–D667 (2018).

92. P. N. Robinson, S. Köhler, S. Bauer, D. Seelow, D. Horn, S. Mundlos, The human phenotype ontology: A tool for annotating and analyzing human hereditary disease. *Am. J. Hum. Genet.* **83**, 610–615 (2008).

93. K. Yokogami, S. Yamashita, H. Takeshima, Hypoxia-induced decreases in SOCS3 increase STAT3 activation and upregulate VEGF gene expression. *Brain Tumor Pathol.* **30**, 135–143 (2013).

94. A. Stahl, J.-S. Joyal, J. Chen, P. Sapieha, A. M. Juan, C. J. Hatton, D. T. Pei, C. G. Hurst, M. R. Seaward, N. M. Krah, R. J. Dennison, E. R. Greene, E. Boscolo, D. Panigrahy, L. E. H. Smith, SOCS3 is an endogenous inhibitor of pathologic angiogenesis. *Blood* **120**, 2925–2929 (2012).

95. I. Tirado-Hurtado, W. Fajardo, J. A. Pinto, DNA damage inducible transcript 4 Gene: The switch of the metabolism as potential target in cancer. *Front. Oncol.* **8**, 106 (2018).

96. J. L. Ebersole, M. J. Novak, L. Orraca, J. Martinez-Gonzalez, S. Kirakodu, K. C. Chen, A. Stromberg, O. A. Gonzalez, Hypoxia-inducible transcription factors, HIF1A and HIF2A, increase in aging mucosal tissues. *Immunology* **154**, 452–464 (2018).

97. X. Jiang, W. Tian, A. B. Tu, S. Pasupneti, E. Shuffle, P. Dahms, P. Zhang, H. Cai, T. T. Dinh, B. Liu, C. Cain, A. J. Giaccia, E. C. Butcher, M. C. Simon, G. L. Semenza, M. R. Nicolls, Endothelial hypoxia-inducible factor-2α is required for the maintenance of airway microvasculature. *Circulation* **139**, 502–517 (2019).

98. S. Wingett, P. Ewels, M. Furlan-Magaril, T. Nagano, S. Schoenfelder, P. Fraser, S. Andrews, HiCUP: Pipeline for mapping and processing Hi-C data. *F1000Research* **4**, 1310 (2015).